ionic strengths essentially all the solvent reorganization that is required for electron transfer occurs after formation of the precursor complex. In contrast, the present findings suggest that a sizable solvent contribution to the overall activation free energy arises from the formation of the precursor complex from the separated reactants, although the estimates of ΔG^{W}_{s} obtained from eq 6 and 6a will be markedly too large if nonadiabatic and anharmonic factors are indeed important. Whatever the detailed reasons for the observed behavior, it seems plausible that specific solvation factors can play an important role in determining the kinetics of cationic redox reactions in aqueous solution. The further acquisition of kinetic and thermodynamic data, both in solution and at electrode surfaces, for redox reactions involving systematic variations in ligand structure and thermodynamic driving force should provide valuable additional information on this important question.

Acknowledgment. Dr. Norman Sutin and Professor Henry Taube kindly made available manuscripts in advance of publication. E.L.Y. was partially supported by a summer fellowship from funds made available from the General Electric Corp. The support of this work by the Air Force Office of Scientific Research is gratefully acknowledged.

Registry No. Co^{3+}, 22541-63-5; Co^{2+}, 22541-53-3; Fe^{3+}, 20074-52-6; Fe^{2+}, 15438-31-0; Ru^{3+}, 22541-88-4; Ru^{2+}, 22541-59-9; V^{3+}, 22541-77-1; V^{2+}, 15121-26-3; Eu^{3+}, 22541-18-0; Eu^{2+}, 16910-54-6; Cr^{3+}, 16065-83-1; Cr^{2+}, 22541-79-3; Yb^{3+}, 18923-27-8; Yb^{2+}, 22541-96-4; U^{4+}, 16089-60-4; U^{3+}, 22578-81-0; Np^{4+}, 22578-82-1; Np^{3+}, 21377-65-1; $Ru(NH_3)_6^{3+}$, 18943-33-4; $Ru(NH_3)_6^{2+}$, 19052-44-9; $Ru(en)_3^{3+}$, 21393-87-3; $Ru(en)_3^{2+}$, 21393-86-2; $Co(en)_3^{3+}$, 14878-41-2; $Co(en)_3^{2+}$, 23523-25-3; $Co(phen)_3^{3+}$, 18581-79-8; $Co(phen)_3^{2+}$, 16788-34-4; $Co(bpy)_3^{3+}$, 19052-39-2; $Co(bpy)_3^{2+}$, 15878-95-2; $Ru(bpy)_3^{3+}$, 18955-01-6; $Ru(bpy)_3^{2+}$, 15158-62-0; $Ru(NH_3)_5py^{3+}$, 33291-25-7; $Ru(NH_3)_5py^{2+}$, 21360-09-8.

Contribution from the Departments of Chemistry, University of Vermont, Burlington, Vermont 05405, State University of New York, Albany, New York 12222, and University of North Carolina, Chapel Hill, North Carolina 27514, and the Inorganic Chemistry Laboratory, Oxford University, Oxford OX1 3QR, England

Solid-State Structure and Electronic Properties of a Mixed-Valence Two-Dimensional Metal, KCu_4S_3

DAVID B. BROWN,*[1a] JON A. ZUBIETA,[1b] P. A. VELLA,[1b] JAMES T. WROBLESKI,[1a] TIMOTHY WATT,[1a] WILLIAM E. HATFIELD,[1c] and PETER DAY[1d]

Received November 5, 1979

KCu_4S_3, prepared by the high-temperature reaction of copper, potassium carbonate, and sulfur, crystallizes with a unique layered structure. Double layers of tetrahedrally coordinated (by S) copper ions are separated by layers of potassium ions. Although formally a mixed-valence Cu(I, I, I, II) complex, all copper ions are crystallographically equivalent. Consistent with its Robin and Day class III designation, KCu_4S_3 exhibits electrical conductivity characteristic of a metal. Room-temperature compaction conductivities of ca. 4000 Ω^{-1} cm^{-1} increase to ca. 60 000 Ω^{-1} cm^{-1} at 20 K. The metallic nature of this two-dimensional material is supported by the temperature-independent paramagnetism and the metallic reflectivity through the visible and near-ultraviolet region of the spectrum.

Introduction

In recent years there has been an intensive search for new materials which exhibit high electrical conductivity. Several factors motivate research in this area, including the desire to find new materials with high superconducting transition temperatures. This has been approached by both systematic modifications of known types of superconducting materials and also by the search for new types of superconducting materials, particularly the elusive "excitonic" superconductor.[2] At a more fundamental level, activity in the field has been sustained by the discovery of several new classes of conducting materials, most specifically the one- and two-dimensional conductors which have proven so important in our understanding of the electrical properties of solids.

One class of compounds which have been widely studied are the transition-metal chalcogenides, typified by TaS_2, which crystallize with layer structures.[3] Although most common with the early transition metals, a large number of compounds are known which have certain structural similarities, namely, strong covalent metal–sulfur bonding within a two-dimensional sheet and either weak (van der Waals) or ionic interactions between layers. Many of these materials exhibit either metallic (TaS_2) or semiconducting (MoS_2) electrical behavior, and in each case the properties are highly anisotropic. For example, one crystalline modification of TaS_2 exhibits metallic conductivity in the layers but semimetal or semiconducting behavior perpendicular to the layers, with an anisotropy in the resistivity as high as 500 at low temperatures.[4] Many of these materials exhibit superconductivity at low temperature. Several of these compounds are susceptible to chemical modification. TaS_2, for example, reacts either with organic bases such as pyridine (py) or with alkali metals by intercalation. The lattice expands perpendicular to the planes in order to accommodate the intercalate between the layers. Although the magnitude of the parallel conductivity does not vary greatly in such materials, both the anisotropy in the conductivity and the superconducting transition temperature do change. Thus, the metal sulfides and their ternary intercalates provide a rich area for examining high two-dimensional conductivity.

Although layered structures are relatively common among the sulfides of the early transition metals, the later members of the transition series such as copper tend to form sulfides where three-dimensional interactions prevail. We were intrigued by the report[5] that KCu_4S_3 adopts a layered structure.

(1) (a) University of Vermont. (b) State University of New York at Albany. (c) Univerisity of North Carolina. (d) University of Oxford.
(2) Little, W. A. *Phys. Rev. A* **1964**, *134*, 1416.
(3) Hullinger, F. "Physics and Chemistry of Materials with Layered Structure"; Levy, F., Ed.; D. Reidel: Dordrecht, Holland, 1976; Vol. 5.
(4) Di Salvo, F. J.; Bagley, B. G.; Voorhoeve, J. M.; Waszczak, J. V. *J. Phys. Chem. Solids* **1973**, *34*, 1357.
(5) Rudorff, W.; Schwarz, H. G.; Walter, M. *Z. Anorg. Allg. Chem.* **1952**, *269*, 141.

0020-1669/80/1319-1945$01.00/0

Moreover, the reported structure appears to be unique in that it contains double layers (S–Cu–S–Cu–S) separated by potassium ions. Since the conductivity was reported to be high (40 Ω^{-1} cm^{-1}) there appeared to be physical, as well as structural, similarities to the sulfides of the early transition metals. On the basis of the empirical formulation, KCu_4S_3 is a formally mixed-valence Cu(I, I, I, II) complex. The crystallographic results suggest that all coppers are equivalent, thereby placing the material in the Robin and Day[6] class IIIB. Although there are relatively few materials which may be so designated, they are predicted by theory, and generally found by experiment, to exhibit metallic conductivity. The importance of mixed valence in the design of highly conducting materials has been emphasized recently.[7]

Prompted by the reported properties of KCu_4S_3, we have examined this compound in more detail. The reported structure is based on powder data, and we have carried out a complete single-crystal X-ray structure determination. We also report here the magnetic and electrical properties of KCu_4S_3, including temperature-dependent four-probe conductivity studies, magnetic susceptibility measurements, electronic spectral measurements, and single-crystal conductivity measurements.

Experimental Section

KCu_4S_3 was prepared as described in the literature.[5] Attempts to systematically vary this procedure in order to obtain large single crystals were generally unsuccessful, and there was no apparent correlation between reaction parameters and the quality of the resulting product.

Electrical conductivities for pressed pellets were measured by using two different probe geometries. Pellets were generally pressed at ca. 100 000 psi, although measured conductivities were not sensitive to the pressure used in pellet preparation. Room-temperature conductivities were measured by using a standard in-line four-probe technique with pressure contacts.[8] Commercial probes (Alessi Industries) with both 0.67- and 1.0-mm probe spacings were employed. Measured conductivities were corrected for finite pellet thickness. Measurements were also made by using the van der Pauw technique.[9] A locally designed Teflon sample holder with spring-loaded stainless-steel pressure contacts was used for these measurements. Low temperatures were obtained by suspending this assembly in the Faraday balance shroud of an Air Products Co. Displex CS-202 closed-cycle helium refrigerator. Currents were imposed with a Keithley Model 225 current source and voltages measured with a Keithley nanovoltmeter. Single-crystal conductivities parallel to the two-dimensional sheets of the crystals employed standard probe configurations. Current probes were attached to opposite ends of the crystals by using silver print, and voltage probes were placed on the surface of the crystal by using joy-stick micromanipulators (The Micromanipulator Co., Escondido, CA). Both pressure and silver print contacts were used for the voltage probes.

Magnetic susceptibility data were collected by using a Princeton Applied Research Model 155 vibrating-sample magnetometer (VSM) which was operated at 10 kOe. The VSM magnet (Magnion H-96), power supply (Magnion HSR-1365), and associated field control unit (Magnion FFC-4 with a Rawson-Lush Model 920 MCM rotating-coil gaussmeter) were calibrated against NMR resonances at 10 kOe, and the field set accuracy was found to be better than 0.15%. The magnetometer was initially calibrated against $HgCo(NSC)_4$,[10] and the calibrations were checked against a sample of $(NH_4)_2Mn(SO_4)_2 \cdot 6H_2O$.[11] The results using these two standards agreed to within 2% which represents the upper limits to the uncertainty in the measurements. Powdered samples of the calibrants and compounds used in this study were contained in precision-milled Lucite sample holders. Approximately 150 mg of each was used. Diamagnetic corrections for the constituent atoms were made by using Pascal's constants, and a correction for temperature-independent paramagnetism was estimated from tabulated data.[12–14]

Table I

Crystal Data for KCu_4S_3

tetragonal system	$Z = 1$
systematic absences: none	fw = 389.46
space group: $P4/mmm$, $P422$, $P\bar{4}2m$	$V = 140.8$ (1) Å^3
$a = b = 3.899$ (4) Å	ρ(calcd) = 4.590 g cm^{-3}
$c = 9.262$ (6) Å	ρ(found) = 4.59 (2) g cm^{-3} (pycnometrically in xylene at 20 °C)

Data Collection

cryst dimens: 0.152 × 0.149 × 0.150 mm
μ(Mo Kα) = 170.56 cm^{-1}
reflctns: 311 symmetry-independent reflctns for $2 < 2\theta \leq 50°$

Specular reflectivity measurements were made at room temperature with a Unicam SP700 spectrophotometer equipped with an SP735 reflectance attachment. About a dozen of the small platelike crystals were cemented to a matt-black background to make a reflecting surface 3–4 mm^2. Reflectivity was determined with respect to a polished aluminum disk.

Collection and Reduction of Diffraction Data. KCu_4S_3 crystallizes as square platelets, several of which were mounted along an edge. Preliminary cell dimensions were obtained from Weisenberg and precession photographs of the crystals taken with Cu Kα (λ = 1.5418 Å) radiation. With use of these approximate cell dimensions from the film measurements, 18 reflections with $30° \leq 2\theta \leq 40°$ were accurately centered in the counter window of a Seimens AED quater-circle automated diffractometer. A least-squares procedure was used to obtain a best fit between the observed and calculated values of χ, ϕ, and 2θ for these reflections. The cell parameters and relevant crystal data are presented in Table I. As the photographs showed no systematic absences, the space groups $P4$, $P\bar{4}$, $P4/m$, $P422$, $P4mm$, $P42m$, $P4m2$, and $P4/mmm$ must be considered. The space groups $P4$ and $P4mm$ proved to be inconsistent with the unit-cell contents, while $P\bar{4}$ is inconsistent with the observed intensities for ($hk0$) reflection with $1 + k$ = odd which appear very weak. Of the remaining space groups, $P4/mmm$ was chosen initially as the highest symmetry group which contains the other space groups of the $4/mmm$ Laue symmetry as subgroups. Subsequent successful refinement of the structure in this space group and the failure of refinements in lower symmetry groups to improve the discrepancy factor confirmed the choice of space groups. The equivalence of $F(hkl)$ and $F(khl)$ and the statistical test for centricity confirmed the choice of Laue symmetry $4/mmm$ rather than $4/m$.

Intensity data were collected on a Seimens AED automated diffractometer using Mo Kα radiation filtered through zirconium foil. A scan speed of 1°/min was employed in measuring each reflection by the moving-center/moving-crystal ($\omega/2\theta$) scan method with a scan range of 1.6° in 2θ. A five value measurement was performed on each reflection in the following fashion: the angles were set to the center of the reflection which was then scanned through 0.8° toward negative θ and the count I_1 was recorded; the background was measured for 1.6 min and recorded as I_2; the reflection was scanned through 1.6° toward positive θ and the count I_3 was recorded; the background I_4 on the second side of the peak was counted for 1.6 min; and finally, the peak was scanned back through 0.8° and the count I_5 was recorded. Since the counting times $t_2 + t_4 = t_1 + t_3 + t_5$, the net count is given by the relationship $I(\text{net}) = {}^1/_2[(I_1 + I_3 + I_5) - (I_2 + I_4)]$. The intensities of three standard reflections used to monitor diffractometer and crystal stability fluctuated by ±1.0% over the period of the data collection.

The observed intensities were corrected for background, Lorentz, polarization, and absorption effects. Only reflections with $I > 2.58\sigma(I)$ were included in the refinement. The observed data were not corrected for secondary extinction.

(6) Robin, M. B.; Day P. *Adv. Inorg. Chem. Radiochem.* **1967**, *10*, 248.
(7) Hatfield, W. E., Ed. "Molecular Metals"; Plenum Press: New York, 1979.
(8) Valdes, L. B. *Proc. IRE* **1954**, *42*, 420.
(9) van der Pauw, L. J. *Philips Res. Rep.* **1958**, *13*, 1.
(10) Brown, D. B.; Crawford, V. H.; Hall, J. W.; Hatfield, W. E. *J. Phys. Chem.* **1977**, *81*, 1303.
(11) McKim, F. R.; Wolf, W. P. *J. Sci. Instrum.* **1957**, *34*, 64.
(12) Figgis, B. N.; Lewis, J. In "Modern Coordination Chemistry"; Lewis, J., Wilkins, R. G., Eds.; Interscience: New York, 1960; Chapter 6, p 403.
(13) König, E. "Magnetic Properties of Transition Metal Compounds"; Springer-Verlag: Berlin, 1966.
(14) Weller, R. R.; Hatfield, W. E., submitted for publication.

Table II. Final Positional and Anisotropic Thermal ($\times 10^4$) Parameters[a,b]

atom	x	y	z	U_{11}	U_{22}	U_{33}
Cu	0.5000	0.0000	0.1603 (2)	27.9 (7)	20.7 (6)	24.6 (5)
K	0.0000	0.0000	0.5000	25.6 (12)	25.6	17.3 (15)
S1	0.0000	0.0000	0.0000	18.2 (11)	18.2	12.2 (14)
S2	0.5000	0.5000	0.2944 (3)	18.0 (8)	18.0	12.1 (10)

[a] Estimated standard deviations are given in parentheses. [b] The vibrational coefficients relate to the expression $T = \exp[-2\pi^2 \cdot (U_{11}h^2a^{*2} + U_{22}k^2b^{*2} + U_{33}l^2c^{*2} + 2U_{12}hka^*b^* + 2U_{13}kla^*c^* + 2U_{23}klb^*c^*)]$. $U_{12} = U_{13} = U_{23} = 0.0$ for all atoms.

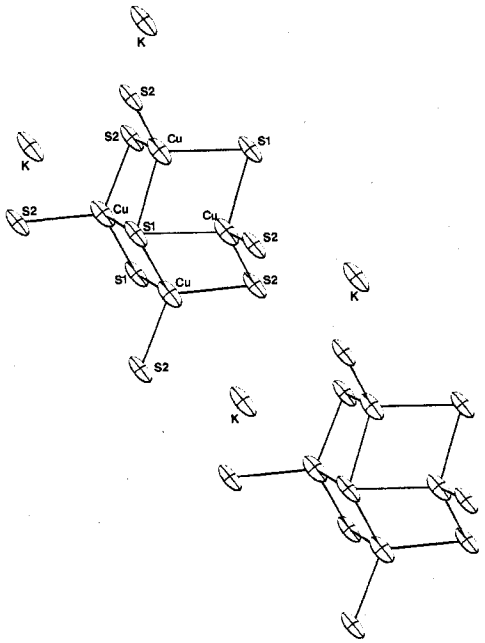

Figure 1. Atom-labeling scheme and the 50% thermal ellipsoids for KCu_4S_3, illustrating the position of the K^+ layers relative to the Cu–S double layers.

Solution and Refinement of the Structure.[15] A sharpened Patterson map was computed by using the corrected data. The map was contoured and solved for the positions of the copper atom and one sulfur atom (R = 32%). The positional coordinates were used to produce a set of phased structure factors for a difference Fourier synthesis which revealed the positions of the potassium and sulfur atoms. The positional and anisotropic thermal parameters of the atoms were refined by a least-squares method for six cycles, leading to convergence at 0.062 and 0.074 for the discrepancy factors $R_1 = \sum||F_o| - |F_c||/\sum|F_o|$ and $R_2 = (\sum w(|F_o| - |F_c|)^2/\sum w|F_o|^2)^{1/2}$, respectively, where the weights, w, were taken as $1/\sigma^2$. Scattering factors for the zerovalent Cu, K, and S atoms were taken from ref 16.

Results. The final positional and thermal parameters for KCu_4S_3 are given in Table II. The pertinent bond lengths and angles are given in Table III. Figure 1 provides the atom labeling scheme and shows the 50% probability ellipsoids for an isolated CuS_4 tetrahedron.

As indicated by the unit cell composition, the atoms must sit at special positions in the cell. The four copper atoms in the cell are located in positions of fourfold multiplicity (Wyckoff position i in $P4/mmm$). The single K atom must sit at a position possessing the full symmetry of the space group, Wyckoff position b in the reference space group, as must S1, which was located at Wyckoff position a. The S2 atoms are at Wyckoff positions g.

Although the empirical formula suggests a species which formally contains both Cu^{1+} and Cu^{2+}, all copper coordination sites are equivalent, with the copper enjoying distorted tetrahedral coordination to the sulfur atoms. The overall structure may be described in terms of double layers built of CuS_4 tetrahedra, the layers being interleaved with K^+ ions surrounded by eight S2 atoms at the vertices of a cube. Figure 2 illustrates the double layers of CuS_4 tetrahedra, generated

(15) The crystallographic programs used in the structure solution and refinement were those compiled in the 1972 version of the X-ray system described by: Stewart, J. M.; Fruger, G. J.; Ammon, H. L; Dickinson, C.; Hall, S. R. Technical Report TR-192, University of Maryland, 1972.
(16) "International Tables for X-Ray Crystallography"; Kynoch Press: Birmingham, England, 1952; Vol. III, pp 202, 204.

Table III. Internuclear Distances, Polyhedral Edge Lengths, and Bond Angles

(i) Interatomic Distances, Å[a,b]

Cu-S1(2)	2.4506 (9)	Cu-K(4)	3.701 (1)
Cu-S2(2)	2.312 (2)	K-S2(8)	3.351 (2)
Cu-Cu(4)	2.7570	K-K(4)	3.899
Cu-Cu(1)	2.970 (2)	S2-S2	3.808 (4)

(ii) Polyhedral Edge Distances, Å

S1-S1	3.899	S1-S2	3.878 (2)
S2-S2	3.899		

(iii) Bond Angles, Deg

Cu-S1-Cu	68.46 (2)	Cu-S2-Cu	73.22 (7)
	74.59 (4)		114.99 (14)
	105.41 (4)	S1-Cu-S1	105.41 (6)
	111.54 (2)	S1-Cu-S2	109.00 (4)
	180.00 (7)	S2-Cu-S2	114.99 (11)

[a] The number of equivalent bonds of a given type is indicated in parentheses. [b] Standard deviations are given in parentheses.

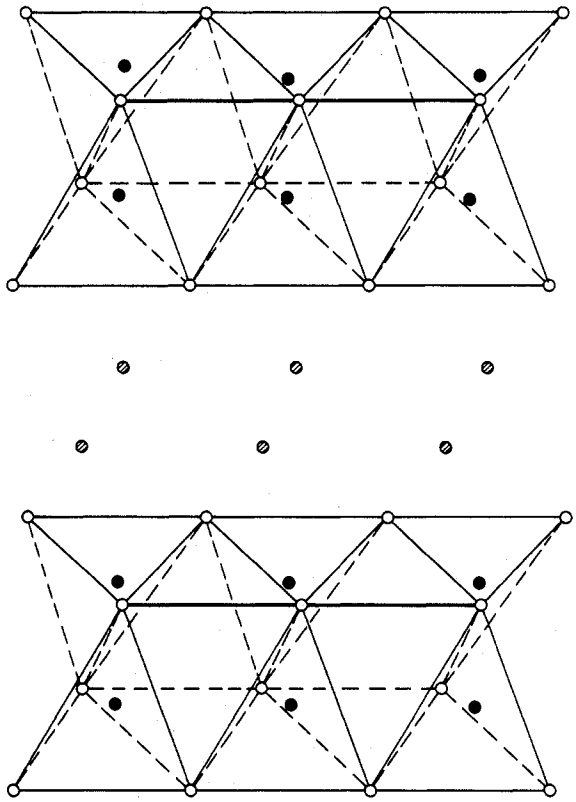

Figure 2. Schematic representation of a portion of adjacent double layers showing the octahedral holes. The shaded circles represent Cu positions, the open circles S, and the crossed circles K.

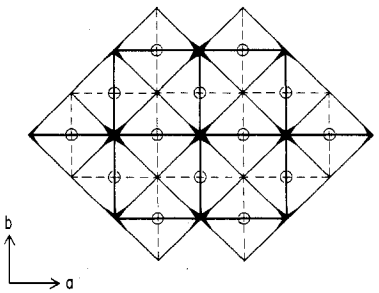

Figure 3. View down the c axis of the edge and vertex-sharing tetrahedra that comprise a Cu–S layer.

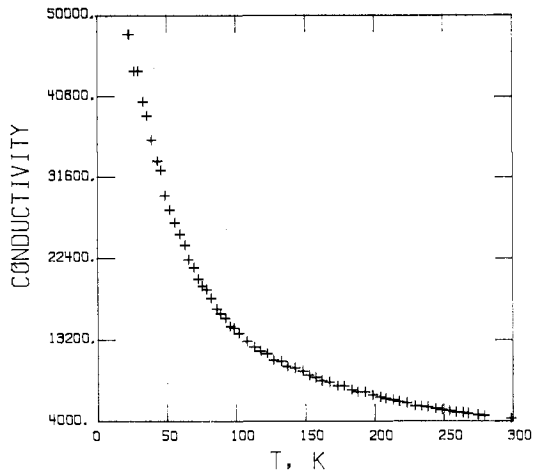

Figure 4. Temperature dependence of the compaction conductivity of KCu_4S_3. Units of conductivity are Ω^{-1} cm^{-1}.

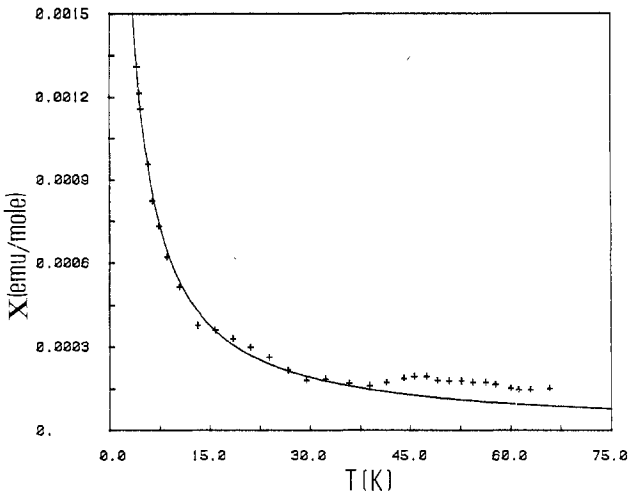

Figure 5. Magnetic data for KCu_4S_3.

by the sharing of five edges and four vertices by each CuS_4 tetrahedron. This diagrammatic representation reveals an unusual feature of the structure, the absence of Cu density at the octahedral sites generated by the sulfur atom packing. A schematic representation of a single layer viewed parallel to the *c* cell axis (Figure 3) shows the edge sharing of CuS_4 tetrahedra with four tetrahedra adjacent in the same layer and the sharing of vertices with two additional polyhedra. A fifth edge is shared with a tetrahedron in the second layer. Sulfur atoms S2 are shared by four tetrahedra, while each sulfur of the central layer, S1, participates in eight polyhedra, with the adjacent Cu atoms at the corners of a cube, at a distance of 2.4506 (9) Å.

It should be emphasized that these structural results are in virtually exact agreement with those obtained nearly 30 years ago from powder diffraction data.[5]

Conductivity

Room-temperature electrical conductivities were measured for six different preparations of KCu_4S_3 by using pressed pellets and four-probe techniques. Measurements were made by using both in-line probes and the van der Pauw technique. In each case, pressure contacts were used. Values of the conductivity obtained by using the in-line probes have been corrected for pellet thickness.[8] Measurements were considered acceptable only after determining that each sample exhibited ohmic behavior. The average value of the room-temperature conductivity, determined from 11 separate experiments, was found to be $\sigma = (4.1 \pm 1.1) \times 10^3\ \Omega^{-1}\ \text{cm}^{-1}$.

The temperature dependence of the conductivity is that of a metal, the resistivity decreasing with decreasing temperature. Figure 4 shows the variation in σ with temperature in the interval 20–300 K. Although not shown in Figure 4, measurements at lower temperatures exhibit a continuing smooth variation. At 20 K the conductivity has risen by a factor of approximately 15 from its room-temperature value to $\sigma \simeq 6 \times 10^4\ \Omega^{-1}\ \text{cm}^{-1}$.

Measurements of the in-plane single-crystal conductivity had a high scatter. This may probably be attributed to the difficulty in obtaining single crystals large enough for accurate placement of electrodes and the difficulty in measuring crystal dimensions. Crystals were always formed as extremely thin fragile plates (ca. 0.03 mm) and were rarely as large as 1 mm^2 on the surface. Average values of the conductivity (13 crystals) within the two-dimensional sheets were found to be $\sigma \simeq 3 \times 10^3\ \Omega^{-1}\ \text{cm}^{-1}$ at room temperature.

Magnetism. The magnetic susceptibility data for KCu_4S_3 in the temperature range 4.2–65 K are shown in Figure 5, where it may be seen that the magnetic susceptibility is largely constant from high temperatures to below 30 K, at which point it begins to increase rather rapidly. When plotted as χ^{-1} vs. temperature, the data below 15 K follow a Curie–Weiss law, $\chi = C/(T - \Theta)$, with $C = 0.00477$ and $\Theta = 0.16$. This behavior is characteristic of the susceptibility of a metallic system with the presence of a low concentration of paramagnetic sites. At high temperature the measured susceptibility is the sum of the Pauli temperature-independent paramagnetism and the Curie–Weiss paramagnetism, while at low temperatures the Curie paramagnetism is dominant. If *g* is taken to be 2.1, a reasonable value for copper(II), the most likely contaminant, then the percent impurity can be estimated from the Curie constant to be 1.4. The Curie–Weiss portion of the paramagnetism calculated from the expression given above was substracted from the measured magnetic susceptibility to give a constant value of 72×10^{-6} emu/mol in the temperature range 40–65 K.

Discussion

Although a large number of copper–sulfide phases are known (Table IV), KCu_4S_3 and its analogues are unique. Most

(17) Berry, L. G. *Am. Mineral* **1954**, *39*, 504.
(18) Buerger, M. J.; Wuensch, B. J. *Science* **1963**, *141*, 276.
(19) O'Keeffe, M.; Hyde, B. G. J. *Solid State Chem.* **1975**, *13*, 172.
(20) Evans, H. T. *Nature (London), Phys. Sci.* **1971**, *232*, 69.
(21) Janosi, A. *Acta Crystallogr.* **1964**, *17*, 311.
(22) Morimoto, N.; Kullerud, G. *Am. Mineral.* **1963**, *48*, 110.
(23) Binnie, W. P.; Redman, M. J.; Mallio, W. J. *Inorg. Chem.* **1970**, *9*, 1449.
(24) Gattow, G. *Acta Crystallogr.* **1957**, *10*, 549.
(25) Flahaut, J.; Domange, L.; Guittard, M.; Ourmitchi, M.; Kam Su Kom, J. *Bull. Soc. Chim. Fr.* **1961**, 2382.
(26) Hahn, H.; de Lorent, C.; Harder, B. *Z. Anorg. Allg. Chem.* **1956**, *283*, 138.
(27) Hahn, H.; Harder, B. *Z. Anorg. Allg. Chem.* **1956**, *288*, 257.
(28) Craig, D. C.; Stephenson, N. C. *Acta Crystallogr.* **1965**, *19*, 543.
(29) Frueh, A. J., Jr. *Z. Kristallogr., Kristallogeom., Kristallphys., Kristallchem.* **1955**, *106*, 299.
(30) Hofmann, W. *Z. Kristallogr., Kristallgeom., Kristallphys., Kristallchem.* **1933**, *84*, 177.
(31) Wuensch, B. J. *Z. Kristallogr., Kristallgeom., Kristallphys., Kristallchem.* **1964**, *119*, 437.
(32) Marumo, F.; Nowacki, W. *Z. Kristallogr., Kristallgeom., Kristallphys., Kristallchem.* **1967**, *124*, 1.
(33) Adiwidjaja, von G.; Lohn, J. *Acta Crystallogr., Sect. B* **1970**, *26*, 1878.
(34) Hultgren, R. *Z. Kristallogr., Kristallogeom., Kristallphys., Kristallchem.* **1933**, *84*, 204.
(35) Azaroff, L. V.; Buerger, M. J. *Am. Mineral.* **1955**, *40*, 213.
(36) Morimoto, N. *Acta Crystallogr.* **1964**, *17*, 351.
(37) Pauling, L.; Brockway, L. O. *Z. Kristallogr., Kristallgeom., Kristallphys., Kristallchem.* **1932**, *82*, 188.

Table IV. Copper–Sulfide Lattices

compd	copper coordination	description of overall structure	bond lengths, Å	ref
CuS	Cu1, trigonal planar, Cu2, tetrahedral	3-D network, two-thirds of S atoms present as S_2^{2-}	2.19 (Cu1–S); 2.32 (Cu2–S)	17
Cu_2S, hexagonal form	Cu1, trigonal planar, Cu2, tetrahedral, Cu3, linear	3-D network, hexagonal close-packed S framework	2.28 (Cu1–S); 2.59 (×3), 2.15 (×1) (Cu2–S); 2.06 (Cu3–S); 2.59 (Cu1–Cu)	18, 19
Cu_2S, monoclinic form	trigonal planar	3-D network, hexagonal close-packed S framework	2.33(mean), 2.88 (Cu–S)	20
$Cu_{1.96}S$	trigonal planar	3-D network cubic closest packing of S atoms	2.31 (Cu–S); 2.64 (×2), 2.97 (×2) (Cu–Cu)	21
$C_{1.8}S$	tetrahedral	3-D network		22
NH_4CuMoS_4	tetrahedral	infinite chain, 2 tetrahedral edges shared	2.31 (3) (Cu–S)	23
$NH_4Cu_7S_4$	trigonal	3-D, cross-linked columns	2.31 (×1), 2.37 (×2) (Cu–S); 2.83 (×4), 2.94 (×1) (Cu–Cu)	24
CuB_5S_8	tetrahedral	spinel structure		25
B = Al			2.34 (Cu–S)	
B = In			2.59 (Cu–S)	
CuB_2S_4	tetrahedral	spinel structure		
B = Cr			2.18 (Cu–S)	26
B = Ti			2.26 (Cu–S)	27
B = V			2.28 (Cu–S)	26
CuAsS	tetrahedral	3-D network of vertex-sharing tetrahedra	2.30 (1), 2.24 (1), 2.34 (1) (Cu–S); 2.416 (6) (Cu–As)	28
CuAgS	trigonal planar	alternate layers	2.29 (×2), 2.26 (×1) (Cu–S)	29
$CuSbS_2$	tetrahedral	3-D network of vertex-sharing tetrahedra	2.25 (×1), 2.29 (×1), 2.33 (×2) (Cu–S)	30
$Cu_{12}Sb_{14}S_{13}$	Cu1, trigonal planar, Cu2, tetrahedral	sphalerite superstructure, vertex-sharing network	2.234 (×1), 2.272 (×2) (Cu1–S)	31
Cu_3AsS_4 I	tetrahedral	zinc blende	2.302–2.337 (1) (Cu–S)	32
II	tetrahedral	wurtzite	2.312–2.323 (Cu1–S)	33
Cu_3VS_4	tetrahedral	3-D, edge-sharing network	2.302–2.381 (Cu2–S); 2.29 (1) (Cu–S)	34
$CuFe_2S_3$	tetrahedral	wurtzite layers with edge-sharing Fe tetrahedra	2.31(av) (Cu–S)	35
Cu_5FeS_4	tetrahedral	3-D network	2.20–2.94 (Cu–S)	36
$CuFeS_2$	tetrahedral	3-D vertex-sharing network, zinc blende superstructure	2.26 (Cu–S)	37
Cu_2FeSnS_4	tetrahedral	derived from $CuFeS_2$ by substitution of $^1/_2$ Fe by Sn atoms	2.31 (Cu–S)	38
KCuS	square planar	zigzag Cu–S chains	2.13 (2), 2.16 (2) (Cu–S); 2.66 (2) (×2) (Cu–Cu)	39
KCu_3S_2	tetrahedral	pleated layers	2.53(mean) (Cu1–S); 2.58(mean) (Cu2–S)	40
$BaCu_4S_3$	trigonal planar, tetrahedral	interwoven copper chains	2.24–2.70 (Cu–S); 2.573–2.965 (Cu–Cu)	41
KCu_4S_3	tetrahedral	double layer, 5 edges/4 vertices shared	2.450 (1) (×2), 2.312 (2) (×2) (Cu–S)	5
			2.757 (×4), 2.967 (×1) (Cu–Cu)	this work

copper sulfides form stoichiometric phases containing, formally, a single oxidation state of copper. The major exception to this generalization is the system $Cu_{2-x}S$, $0 \leq x \leq 0.2$, where a range of nonstoichiometric, and formally mixed-valence, phases are known. By contrast, KCu_4S_3 forms as a discrete mixed-valence system, with no apparent variability in composition, under a variety of experimental conditions. (A different mixed-valence phase, $K_3Cu_8S_6$, forms at higher temperatures.) Under conditions comparable to those used in the preparation of KCu_4S_3, silver forms the singly valent species $K_2Ag_4S_3$.[42]

Although KCu_4S_3 is formally a mixed-valence (nonintegral oxidation state) compound, it is clear from the structural results that all copper ions are equivalent. The material is thus a Robin and Day class IIIB mixed-valence system and as such should have certain predictable physical properties. As discussed below, its conductivity, magnetism, and spectral properties are consistent with this classification.

The three-dimensional structure of KCu_4S_3 is significantly different from those previously reported for copper–sulfide phases of varying compositions. A common feature of the copper–sulfide and more complex phases presented in Table IV is the formation of three-dimensional networks; the occurrence of the double-layer structure appears to be unique to KCu_4S_3 and $RbCu_4S_3$.[5]

The two independent Cu–S distances are similar to those observed previously for tetrahedral Cu–S lattices, which range from 2.13 to 2.59 Å (see Table IV). In addition to the four sulfur neighbors, each copper enjoys close contacts with four coppers at 2.757 Å in the same layer and with one copper at 2.970 (2) Å in the adjacent layer; these copper–copper interactions are similar to those observed in $NH_4Cu_7S_4$[24] where there are four neighbor Cu atoms at 2.83 Å and at 2.94 Å.

As a class IIIB mixed-valence solid, KCu_4S_3 is expected to exhibit metallic conductivity. Indeed, our initial interest in this material was aroused by the report that a compaction of the material exhibited a room-temperature conductivity of 40 Ω^{-1} cm^{-1}. Our work shows that the conductivity is two orders

(38) Brockway, L. O. *Z. Kristallogr., Kristallgeom., Kristallphys., Kristallchem.* **1934**, *89*, 434.
(39) Savelsberg, G.; Schaefer, H. *Z. Naturforsch.* **1978**, *336*, 711.
(40) Burschka, C.; Bronger, W. *Z. Naturforsch.* **1977**, *326*, 11.
(41) Iglesias, J. E.; Pachali, K. E.; Steinfink, H. *Mater. Res. Bull.* **1972**, *7*, 1247.
(42) Bronger, W.; Burschka, C. *Z. Anorg. Allg. Chem.* **1976**, *425*, 109.

of magnitude higher. It is probable that the original measurements used a two-probe technique, and for such a highly conducting material contact resistances would dominate. As expected, the temperature dependence is that of a metal, the conductivity increasing with decreasing temperature. The conductivity exhibits a linear $1/T$ dependence in the temperature range examined.

Although measured with only low precision, the single-crystal conductivity, σ_{11}, is comparable to the bulk conductivity. Assuming highly anisotropic electrical properties, as suggested by the structure, σ_{11} should be larger than the compaction conductivity.[43] The relatively low value for σ_{11} may reflect experimental difficulties in measurements on these single crystals, or it may suggest that the electrical properties are not so highly anisotropic as expected from the structure. Alternatively, the compaction value may be artifically high as a consequence of preferential alignment of these platelike crystals. The fact that bulk conductivities show no significant differences for thoroughly ground samples and direct-crystal compactions suggests that preferential alignment is not a dominant factor.

The value of the conductivity is similar to that of other known metallic materials with layer structures. Thus, σ_{11} for various crystalline modifications of MX_2 (M = Nb, Ta; X = S, Se) is typically 5000–10 000 Ω^{-1} cm^{-1}.[44]

Goodenough[45] has defined a critical internuclear separation, $D_0(n,1)$, which is dependent on the electronic configuration of the metal and the identity of bridging ligands. When metal ion separations are below this critical distance, high mobility collective electrons should be present, and metallic behavior should result. For a d^9 Cu^{2+} complex with sulfide ligands, this distance is predicted to be approximately 3.10 Å. KCu_4S_3, with four Cu–Cu separations of 2.76 Å and one of 2.97 Å, clearly satisfies the Goodenough criterion, and, consequently, its metallic properties are consistent with the theory. Because Cu^{1+}, with a d^{10} electronic configuration, should give rise only to filled bands, metallic conductivity is not expected for materials containing only that oxidation state. Although several Cu^{1+} systems are known ($NH_4Cu_7S_4$, KCuS, KCu_3S_2, $BaCu_4S_3$) which satisfy the Goodenough criterion, electrical properties are apparently known only for $BaCu_4S_3$.[46] This material has a high conductivity (ca. 5 Ω^{-1} cm^{-1}) which is largely temperature independent. There are apparently no known simple Cu^{2+} sulfides. Covellite, CuS, has a nominal Cu^{2+} formulation but is found to contain the ion S_2^{2-} (e.g., $CuS = Cu_2S{\cdot}CuS_2$). Although the oxidation states of copper are distinguishable in that case (Robin and Day class II), the material is metallic. KCu_4S_3 might be predicted to be metallic either as a result of its mixed-valence nature or as a consequence of the Goodenough relations. Apparently neither criterion is sufficient, since $Cu_{1.96}S$ is obviously mixed-valent and has Cu–Cu separations of 2.64 and 2.97 Å yet exhibits semiconducting behavior. It is clear that the relationship between structure and electrical properties in copper sulfides requires further examination.

Magnetism

The Pauli spin magnetization of the conduction electrons in a free-electron gas metal is given[47] by eq 1. Because the

$$M = 3N\mu^2B/2k_BT_F \quad (1)$$

magnetic field induces a diamagnetic component, the total magnetization of a free-electron gas is

$$M = N\mu^2B/k_BT_F = N\mu^2B/E_F \quad (2)$$

where μ is the Bohr magneton (0.921×10^{-20} erg/Oe), B is the magnetic field intensity, k_B is the Boltzmann constant, T_F is the Fermi temperature, and E_F is the Fermi energy. E_F may be estimated from eq 3 where m is the mass of the electron

$$E_F = (\hbar^2/2m)(3\pi^2N/V)^{2/3} \quad (3)$$

and N/V is the conduction electron concentration. For KCu_4S_3, with a single hole in the d-orbital manifold, we expect one carrier per formula unit. Knowing the molar volume (84.85 cm^3), N/V is then 7.1×10^{21} cm^{-3}, and the Fermi energy is calculated as $E_F = 2.19 \times 10^{-12}$ erg. The predicted magnetic susceptibility is then $\chi_\rho = 23.3 \times 10^{-6}$ emu/mol. Since interaction effects tend to increase the susceptibility and since the model assumes the free electron mass, this prediction agrees reasonably well with the oberved susceptibility of $\chi = 72 \times 10^{-6}$ emu/mol.

Reflectivity

In line with their metallic appearance, the reflectivity of KCu_4S_3 crystals in the visible and near-ultraviolet regions was high and almost independent of frequency. There was no sign of a plasma edge over the spectral range studied (roughly 1–4 eV). The simple free-electron band picture predicts a plasma edge given by eq 4. Again assuming the free-electron mass,

$$\lambda_0 = 2\pi[mc^2/4\pi(N/V)e^2]^{1/2} \quad (4)$$

the lack of a plasma edge over the spectral region examined indicates a carrier density greater than about 10^{22} cm^{-3}. This is in reasonable agreement with our expectations of 7.1×10^{21} cm^{-3}, given the formal electronic configurations (d^{10}, d^{10}, d^{10}, d^9) of the four Cu ions.

Conclusion

KCu_4S_3 is a structurally unique material with high (metallic) electrical conductivity. As with other layered conductors, chemical modification by intercalation may be possible, and we are currently pursuing such studies. KCu_4S_3 appears to be only one member of a series of mixed-valence alkali copper sulfides, and it is likely that other reported examples—e.g., $RbCu_4S_3$, $K_3Cu_8S_6$, etc.—will exhibit highly anisotropic metallic conductivity. We will report on these materials at a future date.

Acknowledgment. This work was supported in part by the Office of Naval Research and by a NATO research grant.

Registry No. KCu_4S_3, 60862-03-5.

(43) Kassman, A. J. *J. Appl. Phys.* **1978**, *48*, 2793.
(44) Huntley, D. J.; Frindt, R. F. "Optical and Electrical Properties"; Lee, P. A., Ed.; D. Reidel: Dordrecht, Holland, 1976, p 385.
(45) Goodenough, J. B. "Magnetism and the Chemical Bond"; Interscience: New York, 1963.
(46) Eliezer, Z.; Steinfink, H. *Mater. Res. Bull.* **1976**, *11*, 385.
(47) Kittel, C. "Introduction to Solid State Physics", 5th ed.; Wiley: New York, 1976.